Molecular Neurobiology (2019) 56:567–582
https://doi.org/10.1007/s12035-018-1104-y

Zbtb20 Regulates Developmental Neurogenesis in the Olfactory Bulb and Gliogenesis After Adult Brain Injury

Thorsten R. Doeppner[1] · Josephine Herz[2] · Mathias Bähr[1,3] · Anton B. Tonchev[3,4,5] · Anastassia Stoykova[3,4]

Received: 18 October 2017 / Accepted: 3 May 2018 / Published online: 11 May 2018

Abstract

The transcription factor (TF) Zbtb20 is important for the hippocampal specification and the regulation of neurogenesis of neocortical projection neurons. Herein, we show a critical involvement of the TF *Zbtb20* in the neurogenesis of both projection neurons and interneurons of the olfactory bulb during embryonic stages. Our data indicate that the lack of Zbtb20 significantly diminishes the generation of a set of early-born $Tbr2^+$ neurons during embryogenesis. Furthermore, we provide evidence that *Zbtb20* regulates the transition between neurogenesis to gliogenesis in cortical radial glial progenitor cells at the perinatal (E18.5) stage. In the adult mammalian brain, Zbtb20 is expressed by $GFAP^+$ neural progenitor cells (NPCs) located in the forebrain neurogenic niche, i.e., the subventricular zone (SVZ) of the lateral ventricles. Upon induction of cerebral ischemia, we found that Zbtb20 expression is upregulated in astrocytic-like cells, whereas diminishing the expression levels of Zbtb20 significantly reduces the ischemia-induced astrocytic reaction as observed in heterozygous *Zbtb20* loss-of-function mice. Altogether, these results highlight the important role of the TF *Zbtb20* as a temporal regulator of neurogenesis or gliogenesis, depending on the developmental context.

Keywords Zbtb20 · Olfactory bulb · Post-natal progenitor cell · Astrocyte · Stroke

Introduction

The neocortex of mammals contains numerous neuronal and glial subtypes, predominantly generated during the embryonic (neurons) and perinatal (glia) developmental stages. Both neurons and glia are produced by radial glial stem cells (RGSCs), which reside in the embryonic ventricular zone (VZ), in a specific sequence. Neurogenesis, mostly accomplished during embryogenesis, precedes gliogenesis that occurs at perinatal stages and continues post-natally [1]. The neurogenesis of neocortical layer neurons follows a specific temporal sequence as deep (lower) layer neurons are produced before neuronal subtypes located in superficial (upper) layers [2–4]. The regulation of the sequential generation of layer specific neuronal subsets is not well understood, and to date, only a few genes have been implicated in this process, including chicken ovalbumin upstream promoter-transcription factor (COUP-TF)1 [5, 6], FoxG1 [7], Gli3 [8], Brn2 [9], zinc finger, and BTB domain-containing 20 (Zbtb20) [10]. The precise mechanisms of the transition between neurogenesis and gliogenesis also remain obscure [11]. Some of the known regulators directly induce gliogenesis from the RGSCs. These include transcription factors (TFs), such as nuclear factor IA (NFIA), high-mobility group (HMG) box family member Sox9, Zbtb20 [12–14], as well as Notch signaling [15] and microRNA(miR)-153 [16]. Other factors activate gliogenesis by endowing the RGSCs with a gliogenic competence, including COUP-TF1/2 [6] and miR-17/106 [17].

Electronic supplementary material The online version of this article (https://doi.org/10.1007/s12035-018-1104-y) contains supplementary material, which is available to authorized users.

✉ Anton B. Tonchev
anton.tonchev@mu-varna.bg

✉ Anastassia Stoykova
astoyko@gwdg.de

[1] Department of Neurology, University Medical Center Goettingen, Goettingen, Germany

[2] Department of Pediatrics, University of Duisburg-Essen Medical School, Essen, Germany

[3] Center for Nanoscale Microscopy and Molecular Physiology of the Brain (CNMPB), Goettingen, Germany

[4] RG Molecular Developmental Neurobiology, Max Planck Institute of Biophysical Chemistry, Goettingen, Germany

[5] Department of Anatomy, Histology and Embryology, Medical University-Varna, Varna, Bulgaria

Similar to the neocortex, the olfactory bulb (OB) contains two types of neurons: glutamatergic projection neurons (mitral and tufted cells) and GABAergic interneurons, mostly situated in the granular and glomerular layers (GLs) [18]. In addition, a small population of glutamatergic interneurons exists. Similar to neocortical neurogenesis, the generation of OB neuronal subtypes starts at stage E11 by forebrain VZ RGSCs which first produce the glutamatergic projection neurons in an inside-first-outside-last schedule (mitral cells followed by tufted cells) [19, 20]. Later in development as well as post-natally, a heterogeneous set of glutamatergic periglomerular neurons, marked by the expression of T-Box TFs Tbr1 and Tbr2, are produced [21]. Gradually, the production of glutamatergic neurons slows down, which parallels the arrival into the OB of GABAergic interneurons that are generated mostly from the embryonic dorsal lateral ganglionic eminence (dLGE) [22]. They migrate along the rostral migratory stream (RMS) and incorporate into the OB [23, 24].

The TF Zbtb20 was previously reported to play a critical role in hippocampal neurogenesis and subfield specification [25–29]. Recently, we have revealed an involvement of Zbtb20 in the timely generation of neocortical glutamatergic neuronal subsets [10]. Here, we show that in the OB, Zbtb20 regulates neurogenesis not only of glutamatergic projection neurons but also of the glomerular GABAergic interneurons (INs) and astrocytes. The analysis revealed that at post-natal stages, a high Zbtb20 expression level defines a subpopulation of $GFAP^+$ precursor cells including neural stem cells (NSCs), which respond to ischemic brain injury. Notably, decreased levels of Zbtb20 in transgenic mice lead to a reduced post-stroke gliogenic scar, suggesting a requirement of Zbtb20 for gliogenesis after pathological conditions, such as ischemic brain injury.

Materials and Methods

Animal Experiments

Animals were handled in accordance with the German Animal Protection Law and approved by local authorities. All surgical procedures were performed under isoflurane/N_2O anesthesia, and all efforts were made to minimize suffering. The *Zbtb20* gene targeting and the generation of the transgenic mice have been previously described [28]. The *Zbtb20 knock out* (*KO*) mice lack the functionally important BTB/POZ domain of the protein as well as the first of five zinc fingers, which were replaced by a *lacZ-neomycin* cassette. Therefore, homozygous mutants will be referred to as $Zbtb20^{lacZ/lacZ}$ mice within this study. The specificity of the deletion and the complete loss of Zbtb20 protein have been confirmed as described [22]. The transgenic mice which express the Cre recombinase under the control of the *hGFAP* promoter [30] and the *Rosa-lacZ* reporter strain which carries β-galactosidase (β-gal) as an endogenous marker [31] were previously described.

Cerebral ischemia was induced using middle cerebral artery occlusion (MCAO) as previously described [32]. Briefly, animals were anesthetized (0.8–1.5% isoflurane, 30% O_2, remainder N_2O), and rectal temperature was maintained at 36.5–37.0 °C, employing a feedback-controlled heating system under a continuous control of blood flow changes by means of a laser Doppler flow (LDF) system (Perimed, Sweden). Occlusion of the middle cerebral artery was achieved using a 7–0 silicon coated nylon monofilament (180-μm tip diameter; Doccol, USA), which was withdrawn after 45 min to induce transient cerebral ischemia. LDF recordings continued for an additional 15 min to monitor appropriate reperfusion.

Histological Processing and Immunohistochemistry

Isolated embryos or brains at defined stages were washed in cold phosphate-buffered saline (PBS) and fixed in 4% paraformaldehyde (PFA) overnight at 4 °C. Tissues were rinsed in PBS and processed for standard cryoembedding. Cryosections (16-μm thick) were washed and blocked for 1 h in blocking solution containing a normal serum. Primary antibodies were incubated overnight at 4 °C in the blocking solution. After washing, the sections were incubated with species-specific secondary antibodies from the Alexa series (Invitrogen) in blocking solution for 2 h at room temperature (RT), washed again, and mounted with Vectashield mounting-medium (Vector Labs) containing DAPI. We used the following primary antibodies/dilutions: mouse anti-β-galactosidase (1:200; Promega, Madison, WI), rat anti-BrdU (1:200; Abcam, Cambridge, UK), rabbit anti-calretinin (1:500, Swant, Bellinzona, Switzerland), goat anti-calretinin (1:300, Millipore/Merck Chemicals GmbH, Darmstadt, Germany) mouse anti-CoupTF1 (1:1000; Perseus Proteomics, Tokyo, Japan), rabbit anti-Cux1 (1:250; Santa Cruz, CA, USA), rabbit anti-doublecortin (DCX; 1:400; Abcam), guinea pig anti-doublecortin (1:300; Millipore), chicken anti-GFAP (1:2000; Abcam), rabbit anti-GFAP (1:200; DAKO, Carpinteria, CA, USA), rabbit anti-NG2 (1:300; Millipore), rabbit anti-nNOS (1:5000; Alexis Chemicals; San Diego, CA, USA), mouse anti-TH (1:300; Millipore), rabbit anti-calretinin (1:1000, Swant), rabbit anti-calbindin (1:1000, Swant), and rabbit anti-Zbtb20 (1:100, Sigma-Aldrich, Taufkirchen, Germany). The anti-BrdU antibodies were visualized after pre-treatment of tissues in 2-N HCl at 37 °C for 30 min. The anti-Zbtb20 antibody was used after an antigen retrieval by heating in a microwave (800 W, three times, 5 min each) in a citrate buffer (pH 6.0).

In Situ Hybridization

Whole heads from E12.5 or whole brains from E18.5 or P4 mice were dissected in ice-cold DEPC-treated PBS, fixed in

4% PFA/PBS for 3 h at 4 °C, washed in PBS, and incubated in 25% sucrose overnight at 4 °C. Specimens were sectioned at 16 μm after embedding and freezing in OCT cryomatrix (Leica Microsystems Nussloch GmbH, Wetzlar, Germany). Non-radioactive in situ hybridization was done as described before.

Image Analysis and Quantification

Images were captured with an Olympus BX60 microscope, a Leica DM6000 epifluorescent system, or a laser confocal microscope (Leica SP5). For cell counts in sections from wild type (WT) and homozygous brains, we blindly counted the positive cells within equally sized frames on coded cross sections of somatosensory cortex in WT and mutant mice ($n \geq 3$ per genotype). Laser confocal microscopy was used to verify co-localization of multiple fluorescent signals. We performed Z sectioning at 0.5–1-μm intervals, and optical stacks of at least 10 images were used for analysis, using the Leica Advanced Fluorescence software version 2.3.6. All images were processed with Adobe Photoshop (Version CS2) by overlaying the pictures, adjusting brightness, contrast, and size.

Statistical Analysis

Statistical evaluation was performed by Student's *T* test or one-way ANOVA followed by Tukey-Kramer's post hoc analysis. Statistical significance between control and experimental condition was considered if $p < 0.05$. Data are presented as means ± s.e.m.

Results

Neuronal Defects in OB of Zbtb20$^{LacZ/LacZ}$ Mice

To study possible functions of Zbtb20 in OB morphogenesis, we assessed the morphology and generation of the neuronal subtypes in the OB of the *Zbtb20 KO* mutant mice. The *Zbtb20*$^{LacZ/LacZ}$ mice possessed smaller OBs (Fig. 1A1–A2, Supplementary Fig. 1). DAPI histochemistry revealed a lack of normal columnar structure in the mutant granule cell layer (GrL); the mitral cell layer (MCL) containing early born glutamatergic projection neurons was thickened and the glomeruli in the glomerular layer (GL) were smaller in the mutants as compared to the control OB (Fig. 1A1–A2, insets). In the mutant GL, the ISH signal for the genes *Id2* and *Vglut2*, which mark glutamatergic projection neurons and INs in the OB [21, 33], was substantially decreased (Fig. 1B1–C2), while *Id2* appeared enhanced in the MCL (Fig. 1B1/B2). Furthermore, Tbr2 immunohistochemistry revealed a significant reduction in the density of Tbr2$^+$ cells in the GL and internal plexiform layer (IPL) (Fig. 1D1/D2, arrowheads), whereas increased cell density was detected in the MCL and outer GrL (oGrL) of the mutants (Fig. 1D1–E2, arrows). Similar results were received when we applied immunostaining for the additional mitral cell marker reelin. Tbr2/reelin double-labeling confirmed nearly complete co-localization (Supplementary Fig. 2). It has been shown that both early- and late-born OB interneurons express Tbr2, while interneurons generated at later developmental stages specifically express Tbr1 [34]. Notably, in the OB of the *Zbtb20KO* mice, there was an ectopic accumulation of Tbr1$^+$ cells in the olfactory core, a segment of the RMS (Fig. 1F1/F2, arrows), suggesting a possible migration defect or an altered Tbr1 expression in *Zbtb20* loss-of-function (LOF) mice.

In addition to the disturbances in the glutamatergic neurons of the mutant OB, we also found deficits in GABAergic interneurons. At post-natal stage day 12 (P12), we detected in the GL a reduction in the neurons positive for calretinin (CR) (Fig. 2A1–A3), calbindin (CB) (Fig. 2B1–B3), tyrosine hydroxylase (TH) (Fig. 2C1–C3), and neuronal nitric oxide synthase (nNOS) (Fig. 2D1–D3). We also observed a reduced astrocytic cell density, marked by S100ß (Fig. 2E1–E3). Triple-labeling for CR, nNOS, and TH revealed that CR and nNOS co-express in most cells, while there was no co-labeling of the two markers with TH (Supplementary Fig. 3). Double-labeling for Zbtb20 and periglomerular interneuron markers (CB, TH, and CR) demonstrated that Zbtb20 was not expressed in these major INs populations in the OB at stage P12 (Fig. 3A1–C3; arrows), with the exception of a few CR$^+$ cells which expressed Zbtb20 protein at low levels (Fig. 3B1–B3, < 1% of the CR$^+$ cells in GL). In contrast, nearly all S100β$^+$ astrocytes expressed Zbtb20 in the OB (Fig. 3D1–D3).

In order to determine whether the described defects were generated during embryogenesis, we performed a birthdate analysis of the cells in the OB by pulse-labeling with BrdU at E12.5, E14.5, E16.5, and E18.5 and evaluated quantitatively the number of BrdU$^+$ cells at post-natal stages (Fig. 4). In the GL, we observed a significant reduction of the E12.5-born and E14.5-born cells (Fig. 4A1–B3). In order to study whether the reduction was due to a decrease in the early-generated Tbr2$^+$ cells, we studied the E12.5-born and E14.5-born Tbr2$^+$ cells in the GL and indeed found that both of these populations were reduced (Supplementary Fig. 4). In the MCL, enhanced E12.5-born BrdU$^+$ cells (Fig. 4A3) were consistent with the finding of increased E12.5-born Tbr2$^+$ cells (Supplementary Fig. 4A4), while no change was found in E14.5-born Tbr2$^+$ cells (Supplementary Fig. 4B4) in accordance with the unchanged quantity of E14.5-born BrdU$^+$ cells in this layer (Fig. 4B1–B3). In the GL, a reduction was evident for the E16.5-born cells (Fig. 4C1–C3), while the number of the E18.5-born cells were enhanced (Fig. 4D1–D3). Furthermore, there was a reduction in the E18.5-born cells in GL (Fig. 4D1–D3) and these were identified to be CR$^+$ interneurons (Supplementary Fig. 5). Together, these results suggest that the disturbances in generation of neuronal subtypes

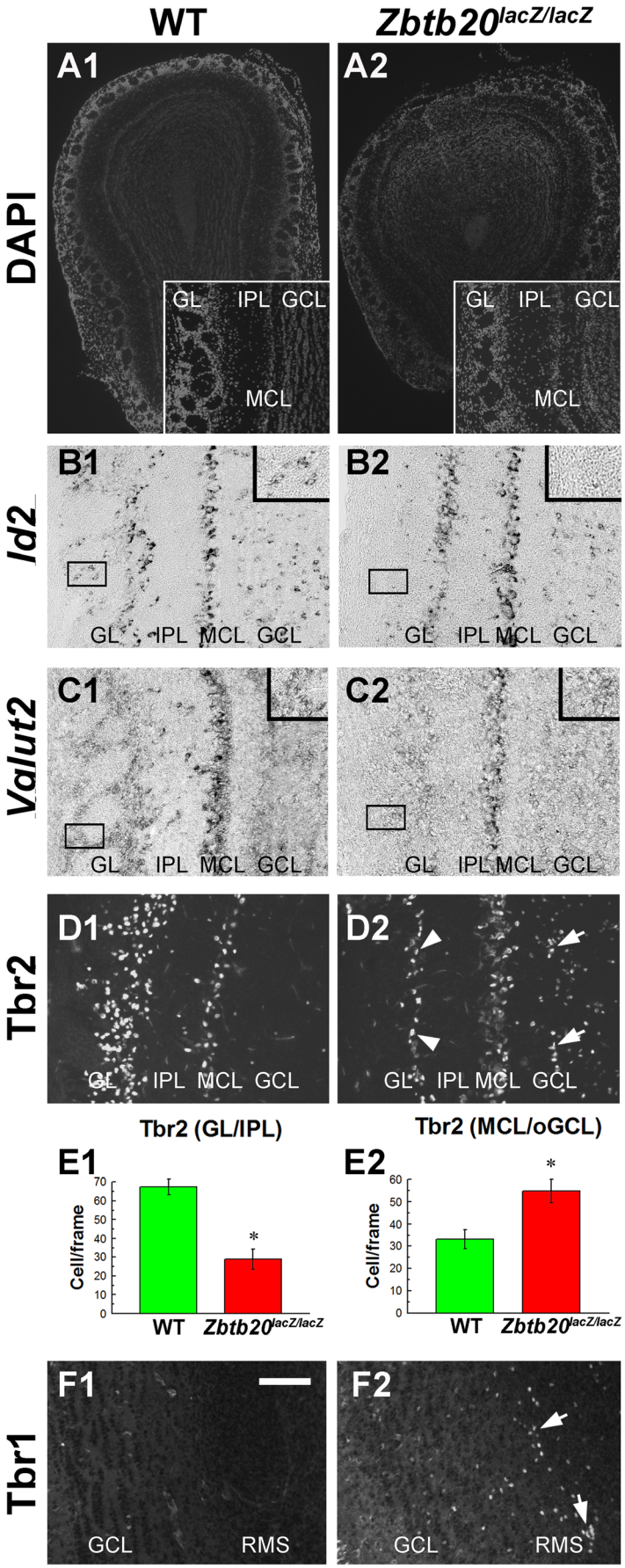

Fig. 1 Defects in olfactory bulb (OB) of Zbtb20$^{LacZ/LacZ}$ mice. **A1**–**A2** DAPI staining of cross sections through the OB of WT and mutants at stage P12 demonstrating the smaller size in the mutant. Inserts depict magnifications demonstrating the layers of the OB. Note the thickened mitral cell layer (MCL). **B1**–**F2** Deficits in glutamatergic neuronal populations in the *Zbtb20* mutant OB. **B1**–**B2** *Id2*$^{+}$ cell ISH signal was decreased in the glomerular layer (GL) in the mutant OB (insets in **B1**–**B2**) but present in the MCL. **C1**–**C2** A decrease in the ISH signal for *Vglut2* in GL in the mutant OB. **D1**–**D2** The Tbr2^{+} cells were decreased in GL (arrowheads), while in the granule cell layer (GCL), they were increased (arrows). **E1**–**E2** Statistical analysis of the number of Tbr2^{+} cells with asterisks indicating a $p < 0.05$. **F1**–**F2** Increased numbers of Tbr1^{+} cells are evident in the mutants' olfactory core, a part of the rostral migratory stream (RMS)

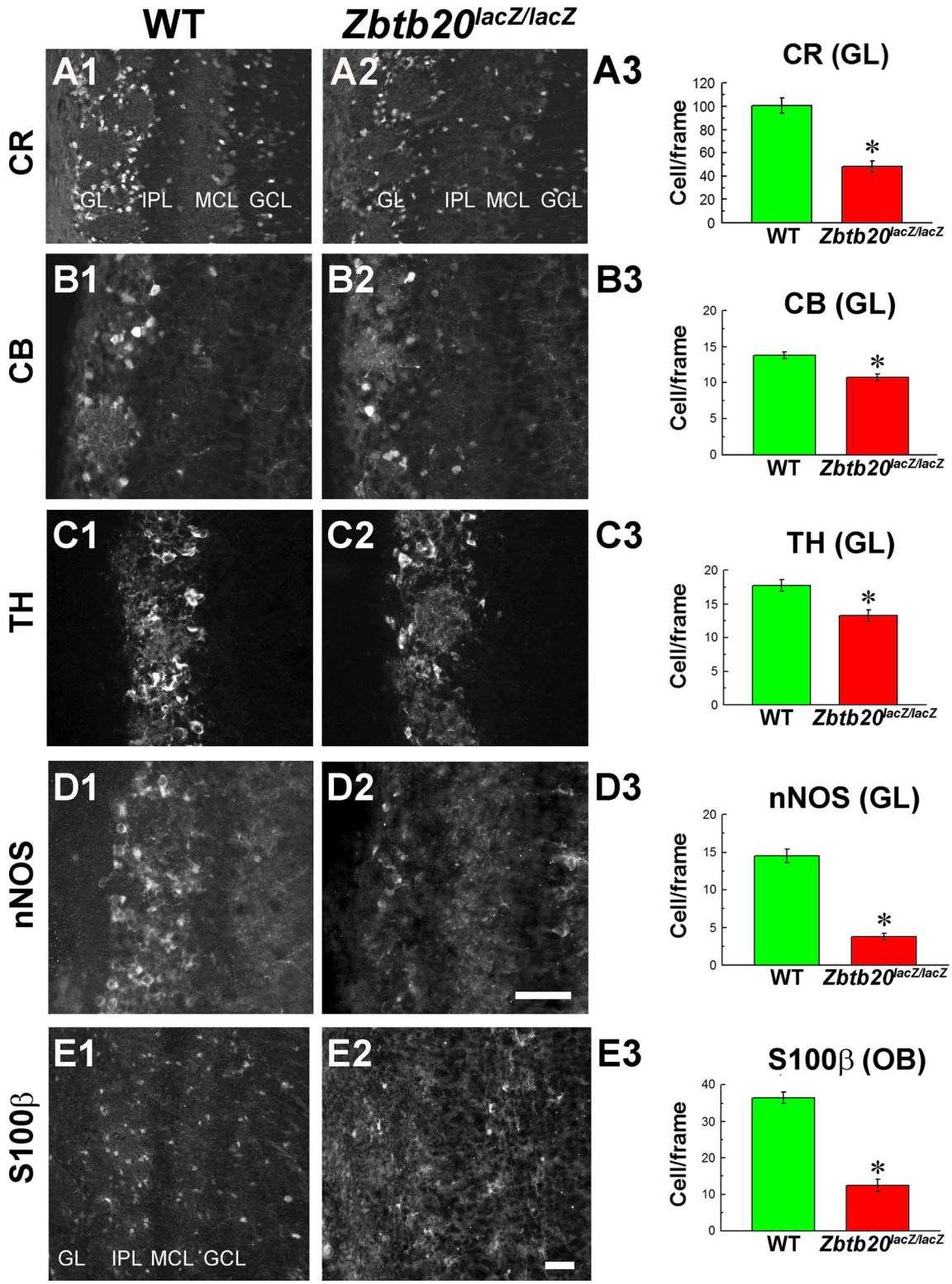

Fig. 2 Deficits in GABAergic interneurons in glomerular layer (GL) of Zbtb20 KO olfactory bulb (OB) at P12. **A1**–**D3** Decreased number of cells in the GL in the mutant OB expressing calretinin (CR) (**A1**–**A2**), calbindin (CB) (**B1**–**B2**), tyrosine hydroxylase (TH) (**C1**–**C2**), neuronal nitric oxide synthase (nNOS; **D1**–**D2**), and statistical analyses, respectively (**A3**, **B3**, **C3**, **D3**). **E1**–**E3** Reduced expression of S100β^{+} cells in both GL and granule cell layer (GCL) of the mutant OB accompanied by a statistical analysis. Asterisks indicate statistical significance with $p < 0.05$. Scale bars: **D2**/**E2**, 50 μm

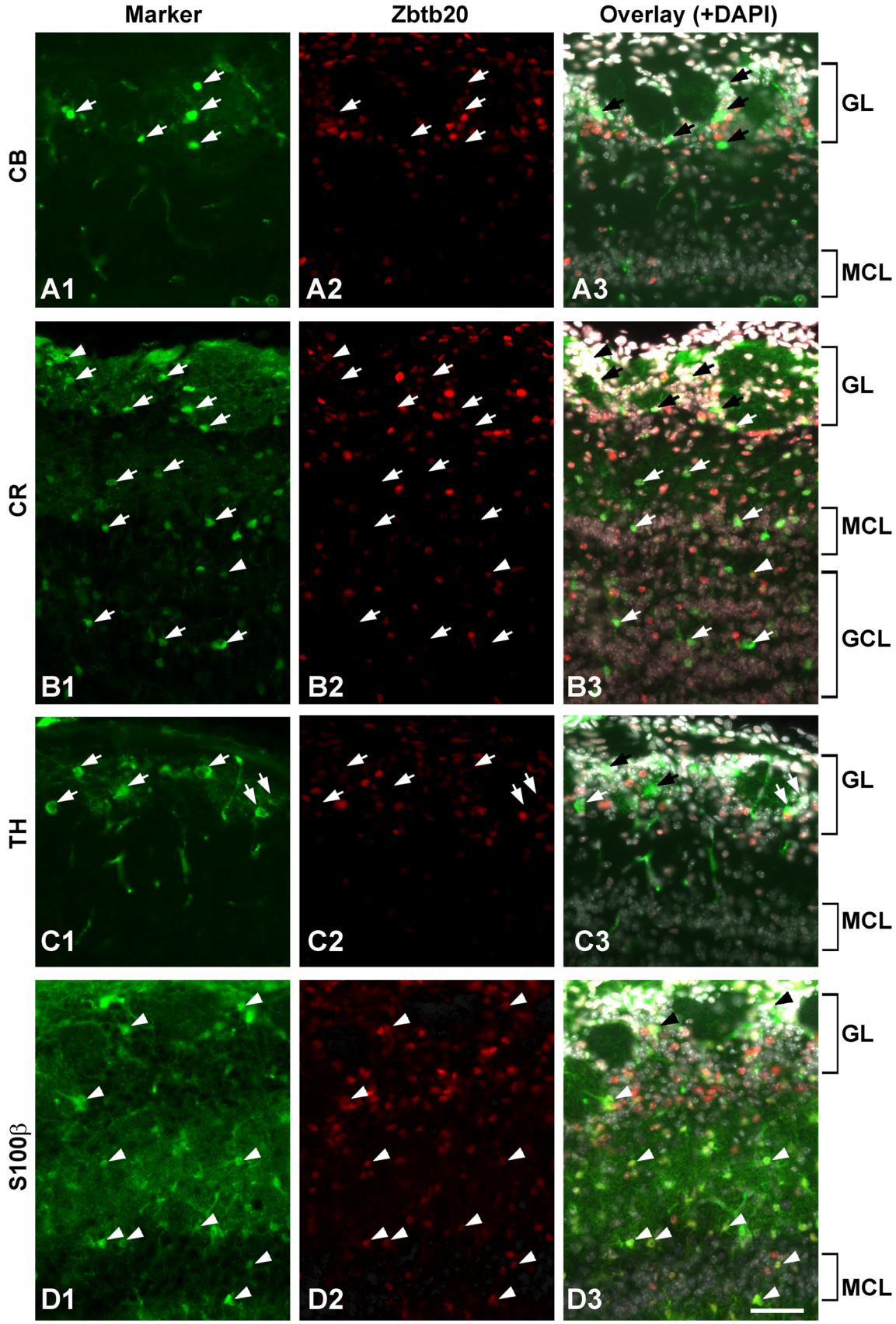
Marker
Zbtb20
Overlay (+DAPI)
CB
CR
TH
S100β
A1
A2
A3
B1
B2
B3
C1
C2
C3
D1
D2
D3
GL
MCL
GCL

◀ **Fig. 3** Post-natal expression of Zbtb20 in neurons and astrocytes of the olfactory bulb (OB) at stage P12. **A1**–**A3** Co-immunostaining with anti-calbindin (CB; arrows) and anti-Zbtb20 antibodies does not show co-labeling. **B1**–**B3** Co-immunostaining for calretinin (CR) and Zbtb20 revealed that most CR^+ cells (arrows) do not co-express Zbtb20. **C1**–**C3** Co-staining between tyrosine hydroxylase (TH; arrows) and Zbtb20 does not show co-labeling as well. **D1**–**D3** Co-staining between the astrocytic marker S100β and Zbtb20 demonstrates co-labeling for many cells (arrowheads). Scale bar: 50 μm

in the OB of *Zbtb20 KO* mice at P12 have mostly occurred during the embryogenesis. To study more deeply the molecular derangements in the OB neurogenesis after *Zbtb20* LOF, we investigated the expression of TFs *Sp8* and *Gsx2*, known to regulate the progenitors of the lateral ganglionic eminence which generate the OB INs [35, 36]. However, we found no change in their expression in the embryonic and early post-natal brain (Supplementary Fig. 6A1–A2 and data not shown). In contrast to this, TFs *ER81* and *Meis2*, which have been implicated in the generation of lately-born OB interneurons [37], were decreased or nearly absent in dorsal LGE at E16.5 in the mutant (Supplementary Fig. 6B1–B2 and data not shown). These results suggest that the prenatally observed neuronal deficits in *Zbtb20 KO mice* might be related to a reduced *ER81* function.

Expression of Zbtb20 Marks Progenitors in the Post-Natal SVZ Stem Cell Niche

Zbtb20 is expressed in the post-natal SVZ of the forebrain lateral ventricle [38], a site of continuous generation of progenitor cells migrating to the OB via the RMS. To gain a deeper insight into the expression of Zbtb20 in the post-natal SVZ neurogenic niche, we performed a detailed analysis of Zbtb20 expression in its cellular components stem-like "B cells," transit amplifying progenitors ("C cells"), and neuroblasts ("A cells") [39]. Based on the expression level of Zbtb20 by IHC, the $Zbtb20^+$ cells in the SVZ can be visually classified as $Zbtb20^+$ cells with a high ($Zbtb20^{hi}$) or a low ($Zbtb20^{lo}$) level of expression (Fig. 5A1, B1, C1; arrows and arrowheads, respectively). We calculated that nearly 60% (73 out of 124) of the $Zbtb20^+$ cells were $Zbtb20^{hi}$ cells, and approximately 40% (51 out of 124 $Zbtb20^+$ cells) were $Zbtb20^{lo}$ cells. Co-localization with GFAP showed that 2/3 (94 out of 142) of the $Zbtb20^{hi}$ cells co-expressed GFAP (Fig. 5A2; arrows), whereas almost none of the $Zbtb20^{lo}$ cells did so (< 1%; Fig. 5A2; arrowheads). Co-staining of Zbtb20 with Ki67, which predominantly stains the C cells, showed that 1/3 (28 out of 82) of the $Zbtb20^{lo}$ cells co-labeled with Ki67 (Fig. 5B1–B2; arrowheads), while only 2% (2 of 92) of the $Zbtb20^{hi}$ cells did so (Fig. 5B1–B2; arrows). Similar results were obtained using Ascl1, an alternative C cell marker (data not shown). Similar to Ki67, double staining of Zbtb20 with DCX, a marker of "A cells" (neuroblasts), resulted in a high percentage of co-expression in the $Zbtb20^{lo}$ cells (93%, 110 of 118 $Zbtb20^{lo}$ cells), while virtually none of the $Zbtb20^{hi}$ cells co-expressed DCX (Fig. 5C1–C2; arrowheads and arrows, respectively). Altogether, these results suggest that the expression level of Zbtb20 is high in the $GFAP^+$ cells, part of which act as NSCs in the adult brain, while its expression gradually decreases in the transit amplifying "C" cells and in the "A" cells (neuroblasts).

In order to test whether or not Zbtb20 is indeed expressed in the fraction of $GFAP^+$ cells which represent NSCs in the SVZ, we infused BrdU for 10 days and performed triple-staining against Zbtb20/GFAP/BrdU 10 days after the last BrdU injection to identify the BrdU label-retaining $GFAP^+$ cells, which potentially represent the slow cycling stem cell fraction [40]. We identified triple-labeled cells (Supplementary Fig. 7), thus strongly supporting that the population of SVZ $GFAP^+$ cells, which include the stem cell population, expresses Zbtb20.

Because of the early post-natal mortality of $Zbtb20^{lacZ/lacZ}$ mice, we could not investigate the effect of *Zbtb20* LOF on adult neurogenesis. The performed analysis of the early post-natal (P4) SVZ/RMS revealed in the mutant a greatly thickened RMS with a strongly reduced GFAP expression (Fig. 6A1–B2, dotted lines) and an accumulation of $GFAP^+$ cells in the SVZ (Fig. 6A1–B2, asterisks). The thickening of RMS was still visible at P12 as depicted by DCX immunostaining (Fig. 6C1–C2, arrowheads), which also revealed clusters of DCX^+ cells in the mutant subcortical WM adjacent to RMS (Fig. 6C2, arrow). Furthermore, we found a decreased immunoreactivity for the oligodendrocyte progenitor marker NG2 in the subcerebral white matter adjacent to RMS (Fig. 6D1–D2) and in the $Olig2^+$ cells in the corpus callosum (WT: 30 ± 2 cells/frame, *Zbtb20* KO: 20 ± 2 cells/frame 100 × 100 μm). Together, these results indicate a reduced gliogenesis in $Zbtb20^{lacZ/lacZ}$ mice soon after the switch between neurogenesis and gliogenesis, suggesting an involvement of Zbtb20 in this process.

We have previously shown a temporal requirement of the Zbtb20 expression in the forebrain embryonic RGSCs regulating the early-born versus late-born neurons [10]. More precisely, we found that in *Zbtb20* LOF, late RGSCs continue to produce deep layer neurons thus diminishing the time window for later born superficial layer neuron generation. In order to test an involvement of Zbtb20 in the neurogenesis-to-gliogenesis switch at stage E18.5, we infused BrdU at E18.5 when late RGSCs produce exclusively glial cells and evaluated the E18.5-born astrocytes using S100β as a marker and the E18.5-born neurons using the UL marker Cux1 [41] (Fig. 7). Consistent with the reduction of $GFAP^+$ cells in the mutants (Fig. 6A1–B2), we found reduced numbers of $S100\beta^+$ cells in the gray matter of the $Zbtb20^{lacZ/lacZ}$ neocortex (Fig. 7A1, A2, B). BrdU birth dating revealed reduced E18.5-born $S100\beta^+$ cells the mutant cortex (Fig. 7A1–A4, C). In contrast, an increased number of E18.5-born $Cux1^+$ neurons was

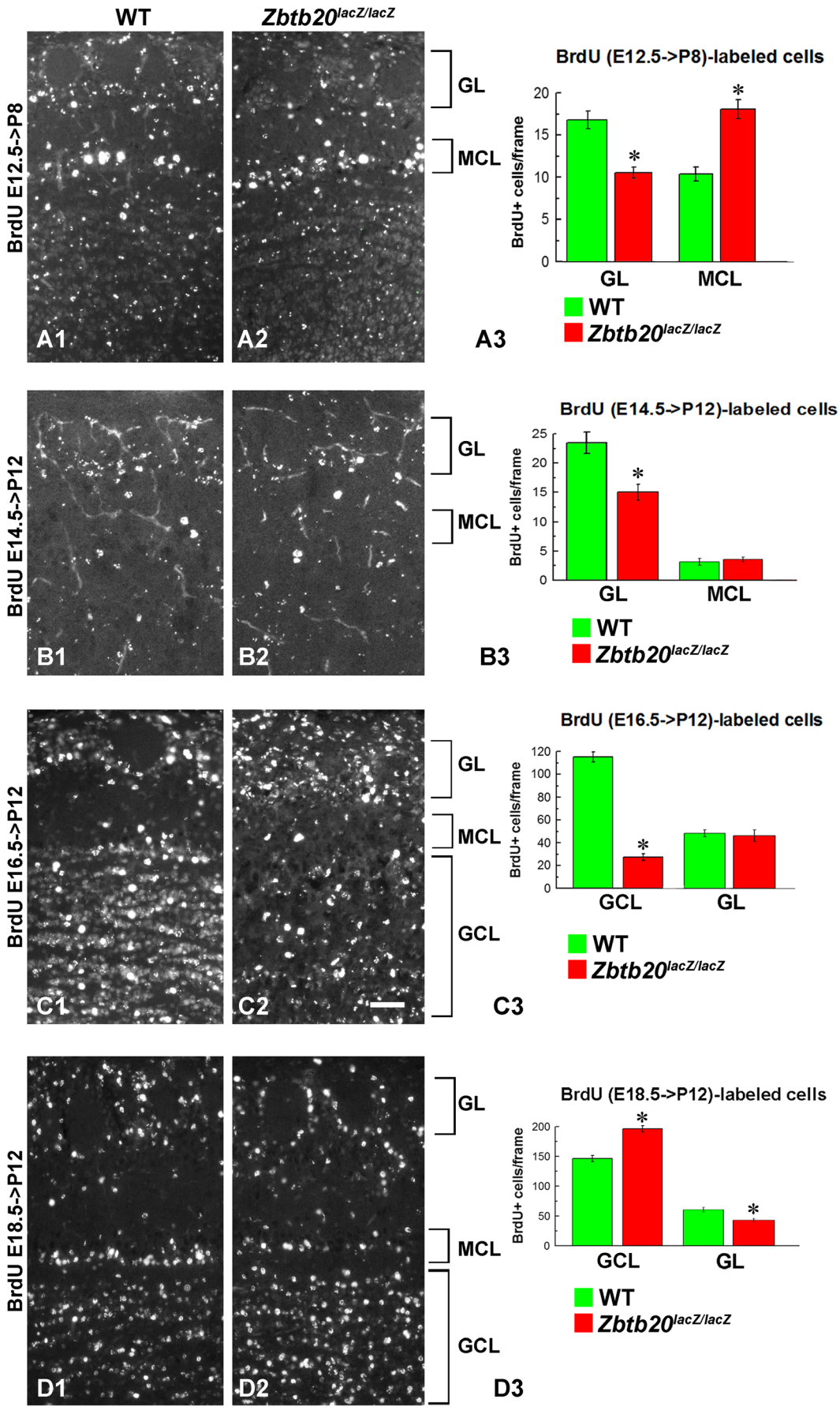
WT
Zbtb20lacZ/lacZ
BrdU E12.5->P8
GL
MCL
A1
A2
A3
BrdU (E12.5->P8)-labeled cells
BrdU+ cells/frame
GL
MCL
WT
Zbtb20lacZ/lacZ
BrdU E14.5->P12
B1
B2
B3
BrdU (E14.5->P12)-labeled cells
BrdU E16.5->P12
GCL
C1
C2
C3
BrdU (E16.5->P12)-labeled cells
BrdU E18.5->P12
D1
D2
D3
BrdU (E18.5->P12)-labeled cells

◀ **Fig. 4** Density and distribution of cells born at E12.5, E14.5, E16.5, and E18.5 located in the olfactory bulb (OB) of WT and Zbtb20$^{lacZ/lacZ}$ mice. Pregnant mice were injected with BrdU at the embryo stage of E12.5 (**A1**–**A3**), E14.5 (**B1**–**B3**), E16.5 (**C1**–**C3**), and E18.5 (**D1**–**D3**). BrdU immunostaining was examined in the cells of the OB at P8 (for labeling at E12.5) or at P12 (for all other BrdU labeling protocols). Labeling at E12.5 revealed increased numbers of proliferating cells in the MCL while being reduced in the GL (**A3**). When labeled at E14.5, the BrdU^{+} cells were also reduced in the GL but unchanged in the MCL (**B3**). BrdU-labeling at E16.5 indicated unchanged numbers of proliferating cells in the GL and a reduced number in the GCL (**C3**). When labeled at E18.5, the GL contained reduced numbers of BrdU^{+} cells and enhanced number of cells in the GCL (**D3**). Asterisks indicate statistical significance with $p < 0.05$. Abbreviations used: MCL—mitral cell layer, GL—glomerular layer, GCL—granular layer. Scale bar: 50 μm

detected in the superficial layers of the mutant cortex (Fig. 7D1–D4, E). The number of early-born (before E18.5) astrocytes in layer 1 of the neocortex of the *Zbtb20 KO* mice was unaffected (Supplementary Fig. 8). Altogether, these results suggest that *Zbtb20* LOF affects perinatally born glial subpopulations including both cortical astrocytes and oligodendroglial progenitor cells.

TF Zbtb20 Is Involved in Post-Ischemic Gliogenesis

Thus far, we have established that Zbtb20 is expressed by post-natal SVZ progenitors including the NSC fraction and that its levels affect the normal developmental genesis of glial populations, in particular astrocytes. The astrocyte response to injury, known as reactive gliosis, is highly prevalent after brain damage but is still poorly understood. Given the potential of Zbtb20 to affect astrocytic levels under normal conditions, we addressed its role under conditions of injury using an experimental stroke model [32]. The application of this model inflicts damage on the ipsilateral striatum and cortex of adult

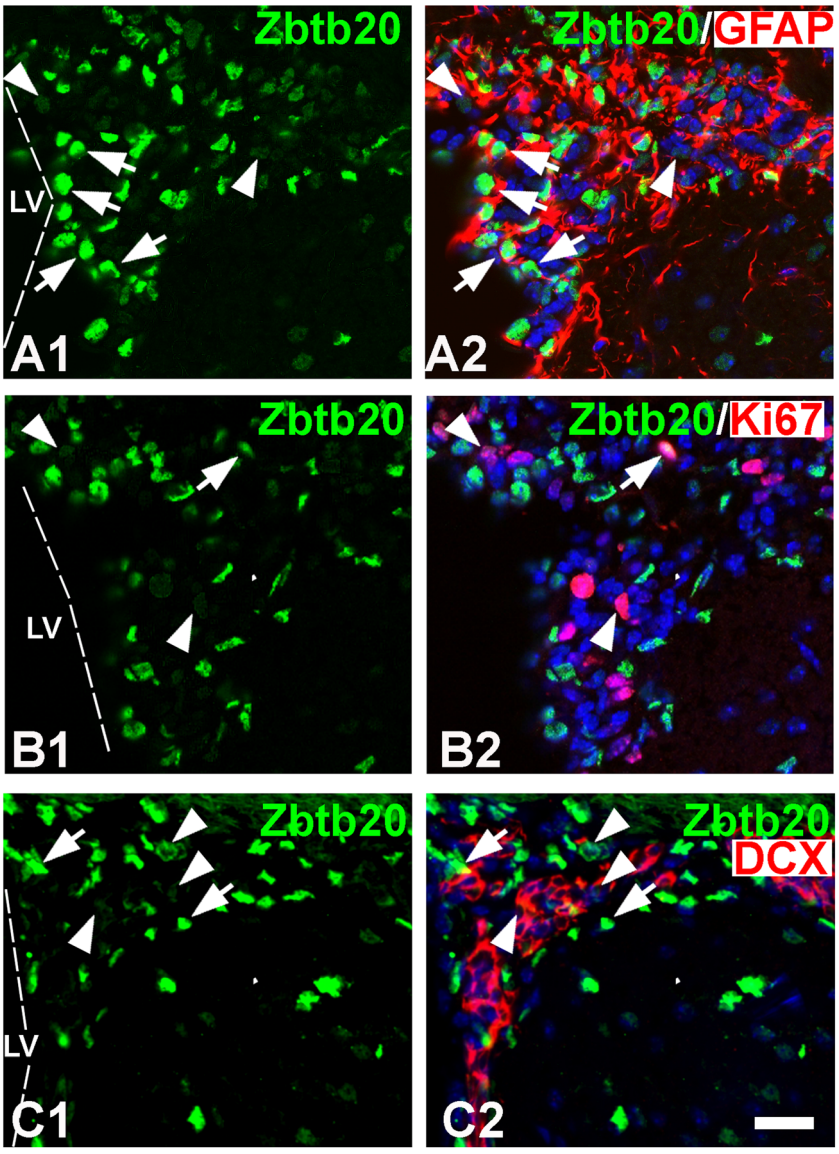

Fig. 5 Expression of Zbtb20 in the adult subventricular zone (SVZ) stem cell niche at stage P30. **A1**–**A2** Double immunolabeling with Zbtb20 (green) and GFAP antibodies demonstrates that Zbtb20^{+} cells with a strong immunoreactivity (Zbtb20^{hi}, arrows in **A1**) are co-labeled for GFAP (arrows, **A2**). On the contrary, the Zbtb20^{+} cells with a low immunosignal (Zbtb20^{lo}, arrowheads in **A1**) do not co-label with GFAP (arrowheads in **A1**). **B1**–**B2** Double-labeling of Zbtb20 with Ki67 depicts that both Zbtb20^{hi} (arrow) and Zbtb20^{lo} (arrowheads) positive cells express Ki67. (**C1**–**C2**) Double-immunostaining of Zbtb20 with DCX shows that most Zbtb20^{hi} cells (arrows) are negative for DCX, while the Zbtb20^{lo} cells (arrowheads) are positive. The images in (**A2**, **B2**, **C2**) are counterstained by DAPI histochemistry. Scale bar: 20 μm

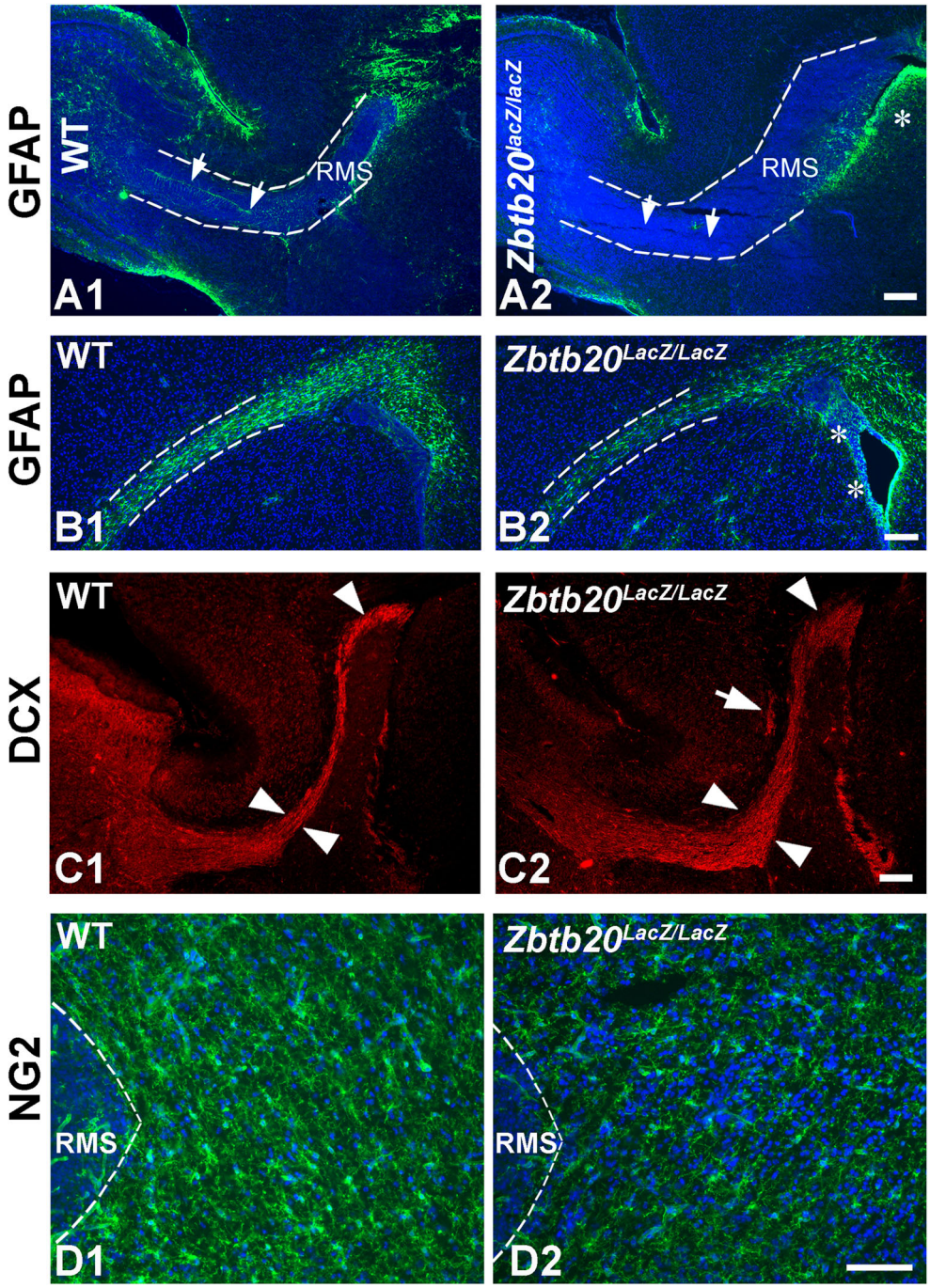

Fig. 6 Effects of Zbtb20 loss-of-function on the early post-natal subventricular zone (SVZ) and on the rostral migratory stream (RMS). **A1**–**A2** The RMS as depicted by DAPI histochemistry (dotted lines) on sagittal brain sections is enlarged in the mutants at P4. This is accompanied by a loss of GFAP (green, arrows) expression within the RMS zone, while there was an accumulation of GFAP$^+$ cells near the ventricles (asterisk). **B1**–**B2** Coronal brain sections at P4 confirm the decrease of the GFAP$^+$ cells in the RMS (dotted line area) and the accumulation of GFAP$^+$ cells in the SVZ (arrows). **C1**–**C2** Sagittal brain sections at P12 demonstrate that the RMS is still more expanded in the mutant (arrowheads) and clumps of DCX$^+$ cells are ectopically located in subcerebral white matter (arrow in C2). **D1**–**D2** Immunostaining for the NG2 proteoglycan at P4 demonstrated a decreased signal in the subcortical white matter adjacent to RMS. The panels in **A1**–**A2**, **B1**–**B2**, and **D1**–**D2** are counterstained for DAPI. Scale bars: **A2**–**C2**, 200 μm; **D2**, 100 μm

mice. After stroke in WT mice, we found a significant increase in the number of Zbtb20$^+$ cells along the ipsilateral SVZ as compared to the contralateral SVZ (Fig. 8A1–A2; insets). Statistical analysis confirmed the significance of this upregulation in the dorsal, lateral, and ventral SVZ (Fig. 8D). Notably, there was a marked increase of the Zbtb20$^+$ cells also in the infarct area (Fig. 8A2; dotted lines) and the ipsilateral pyriform cortex (Fig. 8A2). To study cell proliferation after stroke, we continuously injected BrdU in the operated mice for 10 days starting at day 8 after stroke and sacrificed the animals on day 28 after stroke. We detected a prominent increase of BrdU$^+$ cells in the ipsilateral hemisphere (Fig. 8B1–B2), which paralleled the post-ischemic increase of Zbtb20$^+$ cells in the SVZ (Fig. 8B2; arrow) and the infarct area (Fig. 8B2; dotted lines).

As an additional approach to track whether the progenitor cell response in the SVZ niche after stroke may be related to the Zbtb20 expression, we crossed mice which express the Cre recombinase under the control of the *hGFAP* promoter [30] with the *Rosa-lacZ* reporter strain which carries β-

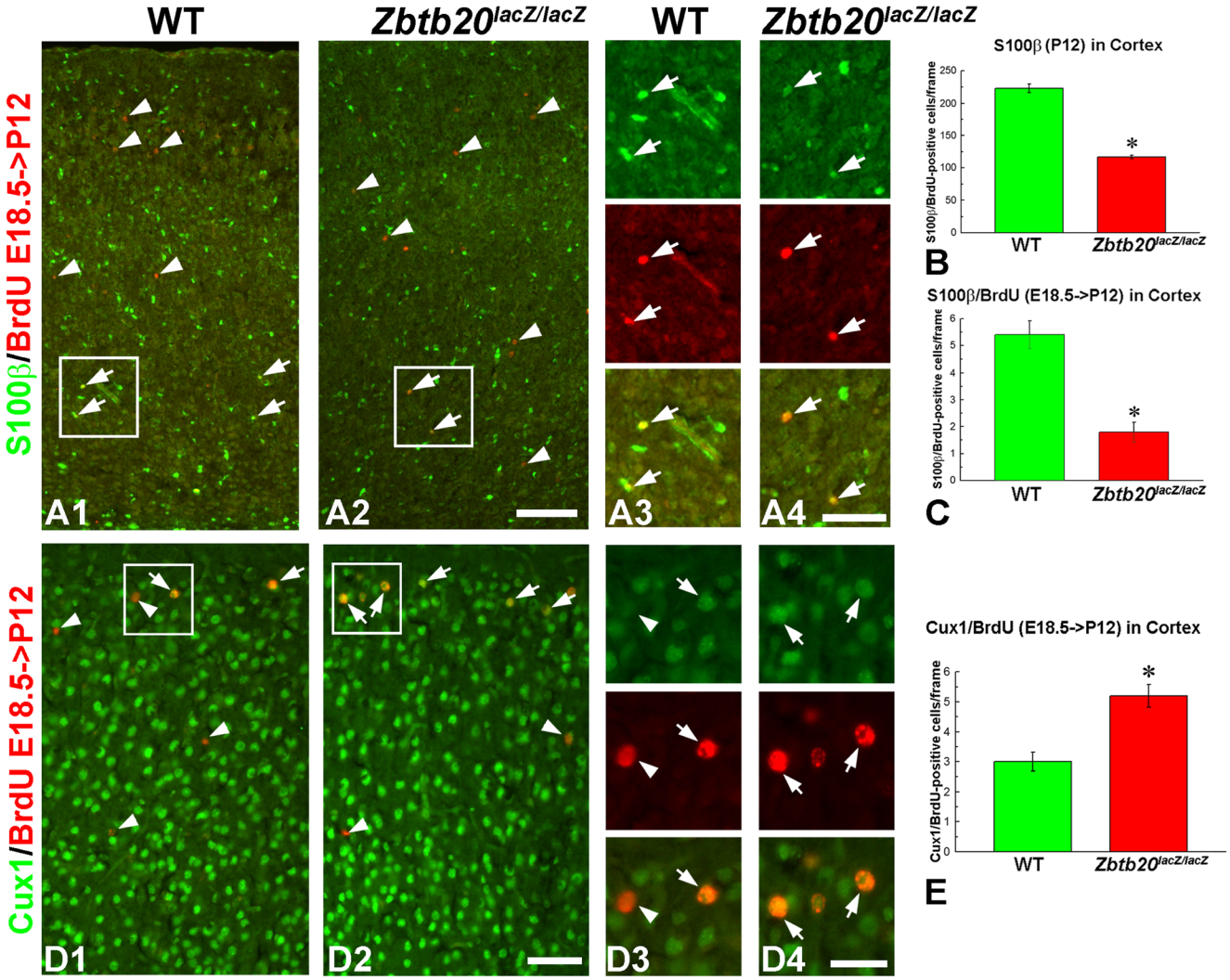

Fig. 7 Diminished presentation of E18.5-born astrocytes in the neocortex of Zbtb20$^{lacZ/lacZ}$ mice. Pregnant mice were injected with BrdU at the embryo stage E18.5, and analysis was performed at P12. **A1**–**A4** Dual staining for S100β (green) and BrdU (red) shows reduction of total S100β$^+$ cells in the cortex as well as a reduction of the E18.5-born S100β$^+$ cell population. Statistical evaluation of the data is presented in panels **B** and **C** with asterisks indicating statistical significance ($p < 0.05$). Frames in **A1** and **A2** correspond to the magnified images of **A3** and **A4**, respectively. **D1**–**D4** Enhanced generation of E18.5-born upper layer neurons positive for Cux1. Dual staining for Cux1 (green) and BrdU (red) shows increase of BrdU$^+$/Cux1$^+$ cells in the uppermost neocortical layers (arrows). Statistical evaluation of the data is presented in panel **E** with asterisks indicating statistical significance ($p < 0.05$). Arrowheads depict BrdU$^+$/Cux1$^-$ cells, typically in deep position. Frames in **D1** and **D2** correspond to the magnified images of **D3** and **D4**, respectively. Scale bars: **A2**/**D2**, 100 μm; **A4**/**D4**, 50 μm

galactosidase (β-gal) as an endogenous marker [31] and performed ischemic injury on the double mutants. At 1 month after stroke, we found an increase of the β-gal$^+$ cells on the ipsilateral side: in the SVZ (Fig. 8C2, arrow), infarct area (Fig. 8C2, arrowhead), and ipsilateral pyriform cortex (Fig. 8C2, black arrowhead). Co-staining of β-gal with Zbtb20 in SVZ and infarct area revealed presence of double-positive cells (Fig. 8E). We then investigated the co-labeling of Zbtb20 with GFAP or DCX in the contralateral and ipsilateral hemispheres upon stroke. We found an upregulation in the double-stained Zbtb20$^+$/GFAP$^+$ cells in the ipsilateral SVZ (Fig. 9A1, arrows) as compared to the contralateral SVZ (Fig. 9A2, arrows). Within the infarct area, most of the Zbtb20$^+$ cells co-labeled with GFAP (Fig. 9B, arrows), whereas only a few cells did not (Fig. 9B, arrowhead). Double-labeling of Zbtb20 with DCX showed increased numbers of double-stained cells in the ipsilateral SVZ (Fig. 9C1, arrows) as compared to the contralateral SVZ (Fig. 9C2, arrow). Statistical evaluation confirmed the significance of the post-ischemic enhancements in the numbers of Zbtb20$^+$/GFAP$^+$ cells and Zbtb20$^+$/DCX$^+$ cells (Fig. 9D).

Due to the early post-natal mortality of *Zbtb20*$^{lacZ/lacZ}$ mice [28, 29], we could not investigate the effect of ischemia on adult homozygous mutant mice. We therefore performed stroke on adult WT and heterozygous *Zbtb20*$^{+/lacZ}$ mice and followed the glial reaction after stroke by means of GFAP

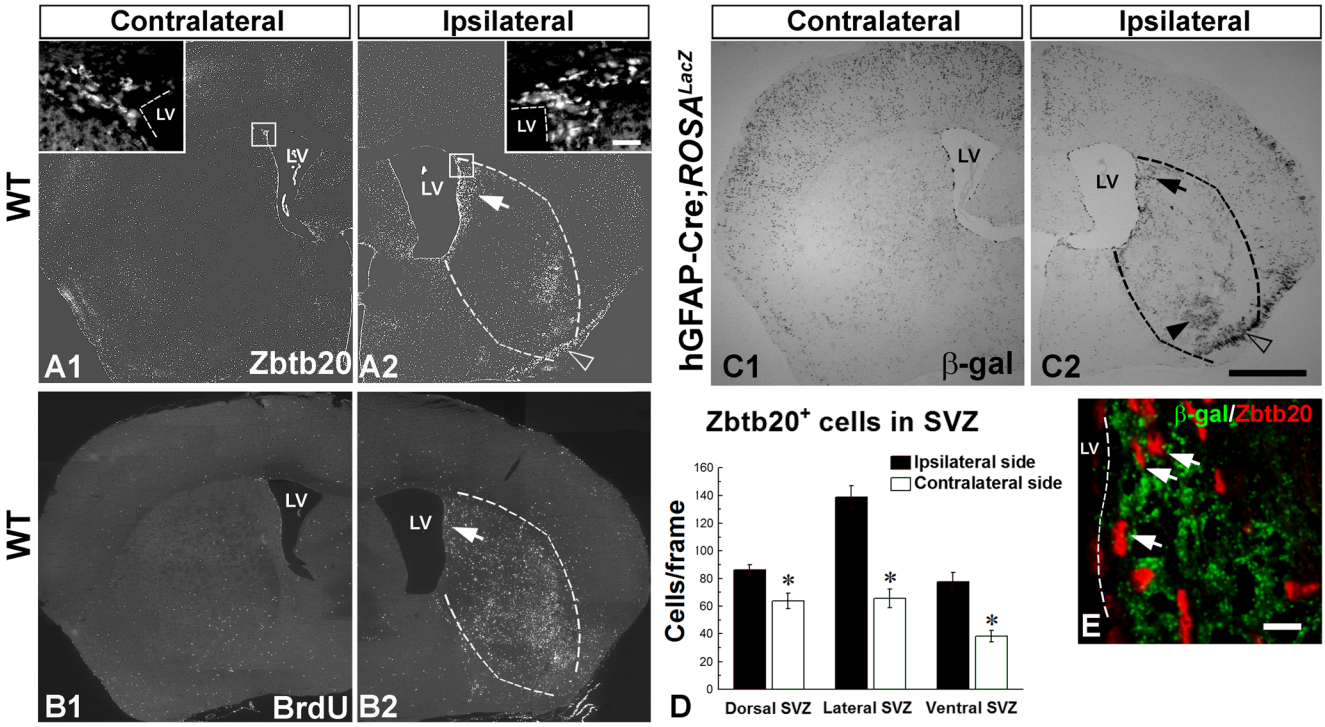

Fig. 8 Enhancement of Zbtb20-expressing cells after focal cerebral ischemia in the adult brain. **A1**–**A2** Effect of brain ischemia on the distribution of Zbtb20$^+$ cells in WT mice ($n = 3$) at P120 after an experimental stroke performed at P90. Low magnification micrographs of contralateral (**A1**) or ipsilateral (**A2**) to stroke hemispheres. Note the increase of Zbtb20$^+$ cells near the ventricle on the ipsilateral side of the damage (arrow in **A2**), in the damaged area in the striatum (infarct borders are outlined by dotted lines) as well as in uppermost layers of the ipsilateral pyriform cortex (empty arrowhead in **A2**). Frames in **A1** and **A2** correspond to the magnified images in the insets depicting the dorsal SVZ. **B1**–**B2** Effect of ischemic stroke on the distribution of cells positive for BrdU. Note the increase on the ipsilateral side which parallels the upregulation of Zbtb20$^+$ cells on the same side. **C1**–**C2** Effect of ischemic stroke on the distribution of cells positive for β-gal in double transgenic *hGFAP*-Cre; *Rosa26*^{lacZ} mice at P120. Stroke was performed on P90 and BrdU was infused daily from P110 to P120. Note the increase of positive cells near the ventricle on the ipsilateral side of the damage (arrow in **C2**), in the damaged area in the striatum (arrowhead in **C2**; infarct borders are outlined by dotted lines) as well as in uppermost layers of the ipsilateral pyriform cortex (empty arrowhead in **C2**). **D** Statistical evaluation of the number of Zbtb20$^+$ cells in dorsal, lateral and ventral SVZ on the ipsi- and contralateral sides of stroke (*, $p < 0.05$). **E** Dual immunofluorescence labeling for Zbtb20 (red) and β-gal (green) in the ipsilateral SVZ. Arrows depict double-positive cells. Scale bars: **C2**, 1 mm; **E**, 10 μm. LV, lateral ventricle

immunolabeling. We found that the heterozygous *Zbtb20*$^{+/lacZ}$ mice exhibited reduced astrocytic reaction (glial scar) in the ipsilateral to the injury hemisphere (Fig. 10B2) as compared to the WT littermates (Fig. 10B1). These findings indicate that TF Zbtb20 is involved in the regulation of the gliogenic reaction to injury.

Discussion

Unlike TFs such as Sp8 [35] and Pax6 [42], which are selectively involved in the neurogenesis of specific OB neuronal populations, we here show that *Zbtb20* LOF affects nearly all OB neuronal types including glutamatergic and GABAergic neurons. The present report is the first to implicate the TF Zbtb20 in OB neurogenesis. Thus, *Zbtb20* LOF leads to derangements not only of glutamatergic [10, 25, 26, 28, 29] but also of GABAergic neurons in the mammalian telencephalon, including the OB.

The enhancement of early-born glutamatergic OB neuronal types in *Zbtb20 KO* mice is in accordance with the increase of early born deep layer neocortical neurons in this mutant [10]. The derangement of the interneuronal populations occurs largely prenatally and is supported by the following evidence: (*i*) expression of Zbtb20 in developing dorsal LGE and septum, the germinative zones of which produce OB INs (42,40); (*ii*) BrdU birthdating analysis showing deficits of generation of INs produced at all tested embryonic stages; and (*iii*) lack of co-expression between Zbtb20 and OB neuronal markers (with the exception of a few CR$^+$ cells) at post-natal stages. Prenatally, we did not detect changes in the expression of TFs *Sp8* (CR$^+$ neurons; [36]), *Gsx2* (LGE and septum-derived interneurons; [35]), and *Pax6* (TH$^+$ interneurons; [42]) in *Zbtb20* LOF, while the expression of TFs *ER81* and *Meis2* [37] was diminished. The molecular mechanisms of embryonically induced deficits in generation of interneurons of OB in *Zbtb20* LOF require further investigation.

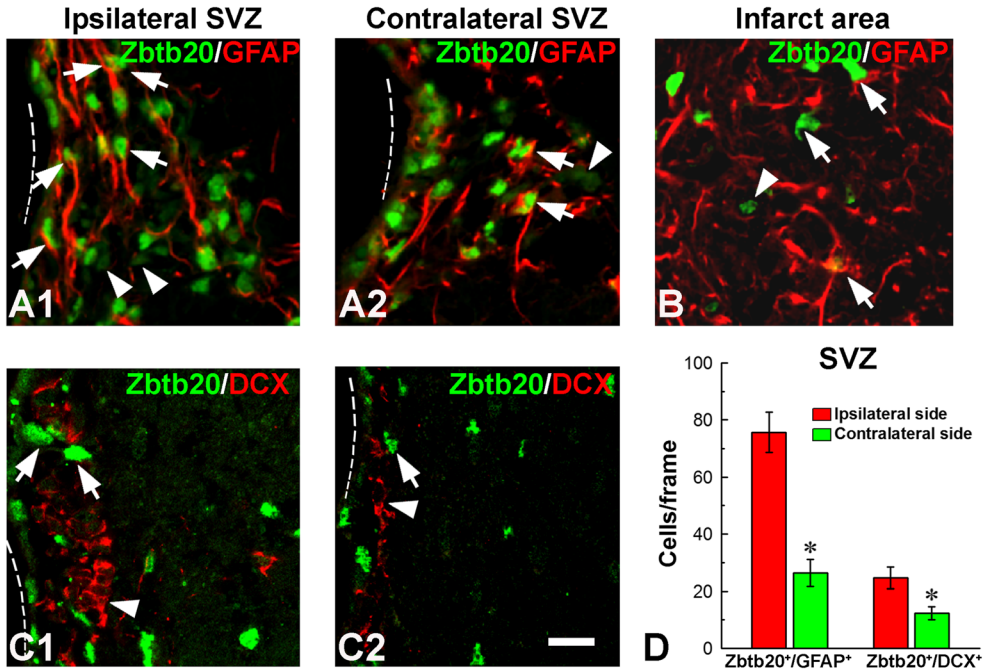

Fig. 9 Phenotype of Zbtb20-expressing cells after stroke. **A1**–**A1** GFAP/Zbtb20 double labeling in ipsilateral (**A1**) or contralateral (**A2**) subventricular zones (SVZ) demonstrates an increased number of double-positive cells in the SVZ on the ipsilateral side. Note that only cells expressing Zbtb20 at a high level (Zbtb20^{hi} cells, arrows) belong to astrocytic lineage, while Zbtb20^{lo} cells do not (arrowheads). **B** Zbtb20/GFAP double labeling in the infarct area shows that most Zbtb20^{+} cells co-express GFAP (arrows). A Zbtb20^{+}/GFAP^{-} cell is depicted by an arrowhead. **C1**–**C2** Zbtb20/DCX double labeling in ipsilateral (**C1**) and contralateral (**C2**) SVZ demonstrates that despite the increase of DCX^{+} cells on the ipsilateral side, their level of Zbtb20 expression does not change—they remain Zbtb20^{lo} cells (arrowheads), while the Zbtb20^{hi} cells (arrows) do not express DCX. Dotted lines outline the border of the lateral ventricle. **D** Statistics of Zbtb20/GFAP and Zbtb20/DCX double positive cells in ipsilateral and contralateral to stroke SVZ (*, $p < 0.05$). Scale bar: **C2**, 10 μm

In addition to neuronal deficits, we found that the lack of *Zbtb20* also leads to diminishing of the glial cells in the OB, which is in accordance with the data of Nagao et al. [14]. Decrease was also observed in cortical and callosal astrocytes but not in L1 astrocytes suggesting that *Zbtb20* differentially affects astrocyte populations in developing brain. The mechanisms by which Zbtb20 modulates astrocyte levels are possibly via the regulation of the onset of the cortical gliogenic program. At gliogenesis stages, *Zbtb20* inhibits late-born neuronal fate [14, 27] allowing for activation of a gliogenic

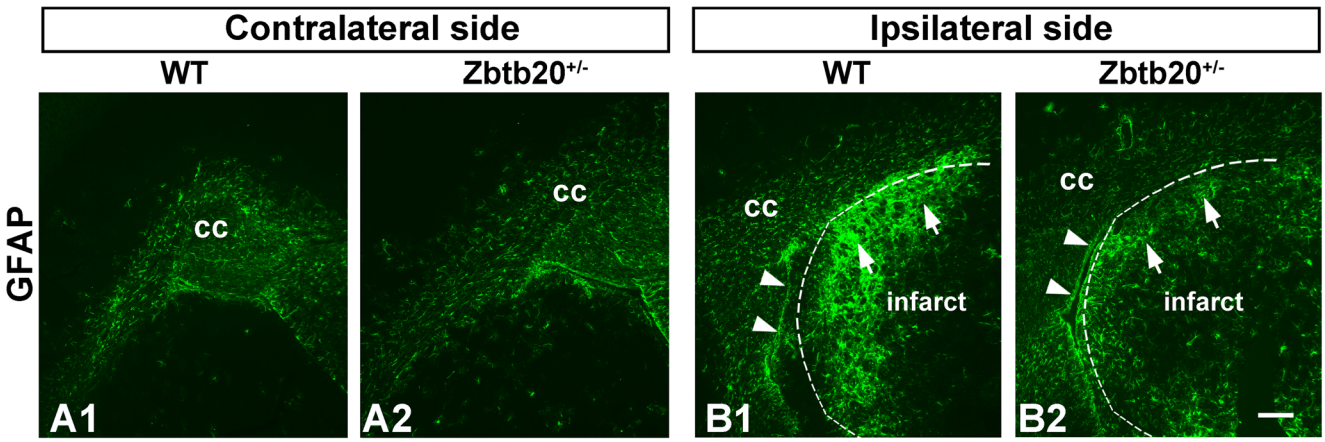

Fig. 10 Reduced glial reaction to stroke in Zbtb20$^{+/lacZ}$ heterozygous mutants. Immunohistochemical staining for GFAP was performed at P120 on cross brain sections from WT or *Zbtb20*$^{+/lacZ}$ heterozygous mutants subjected to stroke experiments at P90 ($n = 3$ per genotype). **A1**–**A2** GFAP staining in the hemisphere contralateral to stroke shows comparable expression levels between WT and heterozygous mutants. **B1**–**B2** In the ipsilateral to the injury hemisphere, the GFAP signal showed an enhanced reaction in both WT (**B1**) and mutant (**B2**) mice. However, the WT mice exhibited an enlarged GFAP-stained area in the striatum (**B1**, arrows) as compared to the striatal parenchyma (**B2**, arrows) of the *Zbtb20*$^{+/lacZ}$ heterozygous animals. The infarct borders are outlined by dotted lines. Arrowheads in (**B1**–**B2**) depict the SVZ. Scale bar: 200 μm

program in RGCs. We herein show that in a lack of *Zbtb20*, the onset of the gliogenic program is delayed and E18.5-born progenitors intensively generate Cux1$^+$ neurons at the expense of glia, leading to an enhanced presence of DCX$^+$ neurons and decreased GFAP$^+$ glia in early perinatal *Zbtb20* LOF telencephalon.

Zbtb20 Expression Identifies a Subset of Post-Natal SVZ Stem Cells Responding to Injury

After midgestation, a subpopulation of RGSCs progressively slows down their cell cycle, becomes quiescent, and contributes to the pool of adult SVZ NSCs [43, 44]. These cells are marked by their strong expression of the astrocyte marker glial fibrillary acidic protein (GFAP) [45] and exert a capacity to generate neurons for cell replacement in the OB of adult mammals [39]. In addition to neurogenesis, the SVZ stem cells are capable of producing oligodendrocytes [46] or astrocytes [47] in the mouse corpus callosum but not in the striatum or the cortex under normal conditions. However, cerebral injury such as stroke is capable of redirecting neuroblasts from their migration to the OB into the affected striatum and cortex [48, 49] or activate a gliogenic program in SVZ progenitors resulting in reactive oligodendrogliogenesis [50] or astrogenesis [51, 52].

Our results provide first data that TF Zbtb20 is expressed by adult SVZ stem cells. The program of adult neurogenesis in the SVZ involves several consecutive steps including division of stem cell-like GFAP$^+$ astrocytes (B cells) in the forebrain SVZ stem niche, followed by generation of transit amplifying (Ki67$^+$/Ascl1$^+$) (C cells), and finally, generation of doublecortin DCX$^+$/βIII-tubulin$^+$ neuroblasts ("A cells") that migrate to OB and regenerate interneurons throughout the life [40]. The stem cell population can be identified by its high expression of GFAP, the retention of BrdU label after long infusion period and by its adherence within the *hGFAP-Cre* lineage [53]. Our analysis revealed that TF Zbtb20, known to predominantly act as a repressor [27], is expressed in the post-natal SVZ niche, showing gradual decrease during the differentiation (B → C → A) of the stem cells. This gradual decrease of Zbtb20 expression in maturating SVZ cells suggests that a successful neuronal differentiation in the post-natal brain might require a decline in Zbtb20 repressive activity. Indeed, we found that DCX$^+$ neuroblasts were enhanced in the absence of Zbtb20 as seen in early post-natal *Zbtb20*$^{lacZ/lacZ}$ mice, while GFAP$^+$ and the gliogenic NG2$^+$ progenitors were reduced. This is consistent with the finding of Nagao et al. [14] and supports their conclusion that in the post-natal brain, Zbtb20 is expressed in a subpopulation of bipotent (astrocytic and oligodendroglial) progenitors.

To obtain a deeper insight into whether the Zbtb20 expression is responsive to a brain injury, we applied a brain stroke model to adult *hGFAP-Cre* reporter which allows a transgenic lineage tracing of SVZ NSCs [54]. Stroke activates SVZ progenitors to produce both neuroblasts and glial cells, but only the glial cell survives in longer periods after the insult [49, 55]. Our analysis indicated a massive enhancement of de novo generated Zbtb20$^+$ cells and an increase of Zbtb20$^+$/GFAP$^+$ cells traced to the β-gal$^+$ lineage along the dorsal, lateral, and ventral SVZ in the ipsilateral side of the stroke. Similarly, the ipsilateral pyriform cortex showed a massive accumulation of Zbtb20$^+$ and hGFAP-Cre lineage cells. Recent data indicate that at this location, some NG2$^+$ progenitor cells reside [56, 57] that are within the hGFAP-Cre lineage [58] and can be activated by cerebral ischemia [59].

To shed light onto the possible functional relevance of the post-natal Zbtb20 expression after a stroke, we applied the MCAO model in heterozygous *Zbtb20*$^{+/lacZ}$ mice, which survive until adulthood. Notably, the heterozygous *Zbtb20*$^{+/lacZ}$ mutants were characterized by a smaller GFAP$^+$ scar in the injured striatum adjacent to SVZ. These findings suggest an involvement of *Zbtb20* in the regulation of the gliogenic response after brain injury. Experiments allowing a conditional elimination of the TF Zbtb20 in the brain SVZ niche are required to define more precisely the function of *Zbtb20* in respect to the regenerative capacity of the adult brain. Interestingly, a recent genome-wide association study identified the *ZBTB20* gene as a risk locus for ischemic stroke in humans [60], thus warranting further investigation of the role of the TF in cerebral ischemia.

Author Contributions A.B.T. and A.S. designed research. A.B.T., T.R.D., and J.H. performed research. T.R.D., A.S., M.B., and A.B.T. analyzed data. T.R.D., A.S., and A.B.T. wrote the manuscript.

Funding Information This work was supported by the Max Planck Society (AS), by the DFG Center for Nanoscale Microscopy and Molecular Physiology of the Brain (CNMPB; AS), TÜBITAK (TRD), and the Alexander von Humboldt Foundation (ABT).

Compliance with Ethical Standards

Competing Interests The authors declare that they have no competing interests.

References

1. Miller FD, Gauthier AS (2007) Timing is everything: making neurons versus glia in the developing cortex. Neuron 54(3):357–369. https://doi.org/10.1016/j.neuron.2007.04.019
2. Angevine JB Jr, Sidman RL (1961) Autoradiographic study of cell migration during histogenesis of cerebral cortex in the mouse. Nature 192:766–768
3. Rakic P (1988) Specification of cerebral cortical areas. Science 241(4862):170–176
4. Takahashi T, Nowakowski RS, Caviness VS Jr (1997) The mathematics of neocortical neuronogenesis. Dev Neurosci 19(1):17–22

5. Faedo A, Tomassy GS, Ruan Y, Teichmann H, Krauss S, Pleasure SJ, Tsai SY, Tsai MJ et al (2008) COUP-TFI coordinates cortical patterning, neurogenesis, and laminar fate and modulates MAPK/ERK, AKT, and beta-catenin signaling. Cereb Cortex 18(9):2117–2131. https://doi.org/10.1093/cercor/bhm238
6. Naka H, Nakamura S, Shimazaki T, Okano H (2008) Requirement for COUP-TFI and II in the temporal specification of neural stem cells in CNS development. Nat Neurosci 11(9):1014–1023. https://doi.org/10.1038/nn.2168
7. Hanashima C, Li SC, Shen L, Lai E, Fishell G (2004) Foxg1 suppresses early cortical cell fate. Science 303(5654):56–59. https://doi.org/10.1126/science.1090674
8. Wang H, Ge G, Uchida Y, Luu B, Ahn S (2011) Gli3 is required for maintenance and fate specification of cortical progenitors. The Journal of neuroscience : the official journal of the Society for Neuroscience 31(17):6440–6448. https://doi.org/10.1523/JNEUROSCI.4892-10.2011
9. Dominguez MH, Ayoub AE, Rakic P (2013) POU-III transcription factors (Brn1, Brn2, and Oct6) influence neurogenesis, molecular identity, and migratory destination of upper-layer cells of the cerebral cortex. Cereb Cortex 23(11):2632–2643. https://doi.org/10.1093/cercor/bhs252
10. Tonchev AB, Tuoc TC, Rosenthal EH, Studer M, Stoykova A (2016) Zbtb20 modulates the sequential generation of neuronal layers in developing cortex. Mol Brain 9(1):65. https://doi.org/10.1186/s13041-016-0242-2
11. Rowitch DH, Kriegstein AR (2010) Developmental genetics of vertebrate glial-cell specification. Nature 468(7321):214–222. https://doi.org/10.1038/nature09611
12. Deneen B, Ho R, Lukaszewicz A, Hochstim CJ, Gronostajski RM, Anderson DJ (2006) The transcription factor NFIA controls the onset of gliogenesis in the developing spinal cord. Neuron 52(6):953–968. https://doi.org/10.1016/j.neuron.2006.11.019
13. Kang P, Lee HK, Glasgow SM, Finley M, Donti T, Gaber ZB, Graham BH, Foster AE et al (2012) Sox9 and NFIA coordinate a transcriptional regulatory cascade during the initiation of gliogenesis. Neuron 74(1):79–94. https://doi.org/10.1016/j.neuron.2012.01.024
14. Nagao M, Ogata T, Sawada Y, Gotoh Y (2016) Zbtb20 promotes astrocytogenesis during neocortical development. Nat Commun 7:11102. https://doi.org/10.1038/ncomms11102
15. Namihira M, Kohyama J, Semi K, Sanosaka T, Deneen B, Taga T, Nakashima K (2009) Committed neuronal precursors confer astrocytic potential on residual neural precursor cells. Dev Cell 16(2):245–255. https://doi.org/10.1016/j.devcel.2008.12.014
16. Tsuyama J, Bunt J, Richards LJ, Iwanari H, Mochizuki Y, Hamakubo T, Shimazaki T, Okano H (2015) MicroRNA-153 regulates the acquisition of gliogenic competence by neural stem cells. Stem Cell Reports 5(3):365–377. https://doi.org/10.1016/j.stemcr.2015.06.006
17. Naka-Kaneda H, Nakamura S, Igarashi M, Aoi H, Kanki H, Tsuyama J, Tsutsumi S, Aburatani H et al (2014) The miR-17/106-p38 axis is a key regulator of the neurogenic-to-gliogenic transition in developing neural stem/progenitor cells. Proc Natl Acad Sci U S A 111(4):1604–1609. https://doi.org/10.1073/pnas.1315567111
18. Parrish-Aungst S, Shipley MT, Erdelyi F, Szabo G, Puche AC (2007) Quantitative analysis of neuronal diversity in the mouse olfactory bulb. J Comp Neurol 501(6):825–836. https://doi.org/10.1002/cne.21205
19. Bayer SA (1983) 3H-Thymidine-radiographic studies of neurogenesis in the rat olfactory bulb. Exp Brain Res 50(2–3):329–340
20. Hinds JW (1968) Autoradiographic study of histogenesis in the mouse olfactory bulb. I. Time of origin of neurons and neuroglia. J Comp Neurol 134(3):287–304. https://doi.org/10.1002/cne.901340304
21. Brill MS, Ninkovic J, Winpenny E, Hodge RD, Ozen I, Yang R, Lepier A, Gascon S et al (2009) Adult generation of glutamatergic olfactory bulb interneurons. Nat Neurosci 12(12):1524–1533. https://doi.org/10.1038/nn.2416
22. Wichterle H, Turnbull DH, Nery S, Fishell G, Alvarez-Buylla A (2001) In utero fate mapping reveals distinct migratory pathways and fates of neurons born in the mammalian basal forebrain. Development 128(19):3759–3771
23. Altman J, Das GD (1965) Autoradiographic and histological evidence of postnatal hippocampal neurogenesis in rats. J Comp Neurol 124(3):319–335
24. Doetsch F, Alvarez-Buylla A (1996) Network of tangential pathways for neuronal migration in adult mammalian brain. Proc Natl Acad Sci U S A 93(25):14895–14900
25. Nielsen JV, Nielsen FH, Ismail R, Noraberg J, Jensen NA (2007) Hippocampus-like corticoneurogenesis induced by two isoforms of the BTB-zinc finger gene Zbtb20 in mice. Development 134(6):1133–1140. https://doi.org/10.1242/dev.000265
26. Nielsen JV, Blom JB, Noraberg J, Jensen NA (2010) Zbtb20-induced CA1 pyramidal neuron development and area enlargement in the cerebral midline cortex of mice. Cereb Cortex 20(8):1904–1914. https://doi.org/10.1093/cercor/bhp261
27. Nielsen JV, Thomassen M, Mollgard K, Noraberg J, Jensen NA (2014) Zbtb20 defines a hippocampal neuronal identity through direct repression of genes that control projection neuron development in the isocortex. Cereb Cortex 24(5):1216–1229. https://doi.org/10.1093/cercor/bhs400
28. Rosenthal EH, Tonchev AB, Stoykova A, Chowdhury K (2012) Regulation of archicortical arealization by the transcription factor Zbtb20. Hippocampus 22(11):2144–2156. https://doi.org/10.1002/hipo.22035
29. Xie Z, Ma X, Ji W, Zhou G, Lu Y, Xiang Z, Wang YX, Zhang L et al (2010) Zbtb20 is essential for the specification of CA1 field identity in the developing hippocampus. Proc Natl Acad Sci U S A 107(14):6510–6515. https://doi.org/10.1073/pnas.0912315107
30. Zhuo L, Theis M, Alvarez-Maya I, Brenner M, Willecke K, Messing A (2001) hGFAP-cre transgenic mice for manipulation of glial and neuronal function in vivo. Genesis 31(2):85–94
31. Soriano P (1999) Generalized lacZ expression with the ROSA26 Cre reporter strain. Nat Genet 21(1):70–71. https://doi.org/10.1038/5007
32. Doeppner TR, Kaltwasser B, Teli MK, Sanchez-Mendoza EH, Kilic E, Bahr M, Hermann DM (2015) Post-stroke transplantation of adult subventricular zone derived neural progenitor cells—a comprehensive analysis of cell delivery routes and their underlying mechanisms. Exp Neurol 273:45–56. https://doi.org/10.1016/j.expneurol.2015.07.023
33. Neuman T, Keen A, Zuber MX, Kristjansson GI, Gruss P, Nornes HO (1993) Neuronal expression of regulatory helix-loop-helix factor Id2 gene in mouse. Dev Biol 160(1):186–195. https://doi.org/10.1006/dbio.1993.1297
34. Winpenny E, Lebel-Potter M, Fernandez ME, Brill MS, Gotz M, Guillemot F, Raineteau O (2011) Sequential generation of olfactory bulb glutamatergic neurons by Neurog2-expressing precursor cells. Neural Dev 6:12. https://doi.org/10.1186/1749-8104-6-12
35. Waclaw RR, Wang B, Pei Z, Ehrman LA, Campbell K (2009) Distinct temporal requirements for the homeobox gene Gsx2 in specifying striatal and olfactory bulb neuronal fates. Neuron 63(4):451–465. https://doi.org/10.1016/j.neuron.2009.07.015
36. Waclaw RR, Allen ZJ 2nd, Bell SM, Erdelyi F, Szabo G, Potter SS, Campbell K (2006) The zinc finger transcription factor Sp8 regulates the generation and diversity of olfactory bulb interneurons. Neuron 49(4):503–516. https://doi.org/10.1016/j.neuron.2006.01.018
37. Allen ZJ 2nd, Waclaw RR, Colbert MC, Campbell K (2007) Molecular identity of olfactory bulb interneurons: transcriptional

codes of periglomerular neuron subtypes. J Mol Histol 38(6):517–525. https://doi.org/10.1007/s10735-007-9115-4
38. Mitchelmore C, Kjaerulff KM, Pedersen HC, Nielsen JV, Rasmussen TE, Fisker MF, Finsen B, Pedersen KM et al (2002) Characterization of two novel nuclear BTB/POZ domain zinc finger isoforms. Association with differentiation of hippocampal neurons, cerebellar granule cells, and macroglia. J Biol Chem 277(9): 7598–7609. https://doi.org/10.1074/jbc.M110023200
39. Lim DA, Alvarez-Buylla A (2014) Adult neural stem cells stake their ground. Trends Neurosci 37(10):563–571. https://doi.org/10.1016/j.tins.2014.08.006
40. Doetsch F, Caille I, Lim DA, Garcia-Verdugo JM, Alvarez-Buylla A (1999) Subventricular zone astrocytes are neural stem cells in the adult mammalian brain. Cell 97(6):703–716
41. Nieto M, Monuki ES, Tang H, Imitola J, Haubst N, Khoury SJ, Cunningham J, Gotz M et al (2004) Expression of Cux-1 and Cux-2 in the subventricular zone and upper layers II–IV of the cerebral cortex. J Comp Neurol 479(2):168–180. https://doi.org/10.1002/cne.20322
42. Dellovade TL, Pfaff DW, Schwanzel-Fukuda M (1998) Olfactory bulb development is altered in small-eye (Sey) mice. J Comp Neurol 402(3):402–418
43. Fuentealba LC, Rompani SB, Parraguez JI, Obernier K, Romero R, Cepko CL, Alvarez-Buylla A (2015) Embryonic origin of postnatal neural stem cells. Cell 161(7):1644–1655. https://doi.org/10.1016/j.cell.2015.05.041
44. Furutachi S, Miya H, Watanabe T, Kawai H, Yamasaki N, Harada Y, Imayoshi I, Nelson M et al (2015) Slowly dividing neural progenitors are an embryonic origin of adult neural stem cells. Nat Neurosci 18(5):657–665. https://doi.org/10.1038/nn.3989
45. Garcia AD, Doan NB, Imura T, Bush TG, Sofroniew MV (2004) GFAP-expressing progenitors are the principal source of constitutive neurogenesis in adult mouse forebrain. Nat Neurosci 7(11): 1233–1241. https://doi.org/10.1038/nn1340
46. Menn B, Garcia-Verdugo JM, Yaschine C, Gonzalez-Perez O, Rowitch D, Alvarez-Buylla A (2006) Origin of oligodendrocytes in the subventricular zone of the adult brain. The Journal of Neuroscience: the Official Journal of the Society for Neuroscience 26(30):7907–7918. https://doi.org/10.1523/JNEUROSCI.1299-06.2006
47. Sohn J, Orosco L, Guo F, Chung SH, Bannerman P, Mills Ko E, Zarbalis K, Deng W et al (2015) The subventricular zone continues to generate corpus callosum and rostral migratory stream astroglia in normal adult mice. The Journal of Neuroscience: the Official Journal of the Society for Neuroscience 35(9):3756–3763. https://doi.org/10.1523/JNEUROSCI.3454-14.2015
48. Zhang R, Zhang Z, Wang L, Wang Y, Gousev A, Zhang L, Ho KL, Morshead C et al (2004) Activated neural stem cells contribute to stroke-induced neurogenesis and neuroblast migration toward the infarct boundary in adult rats. Journal of Cerebral Blood Flow and Metabolism: Official Journal of the International Society of Cerebral Blood Flow and Metabolism 24(4):441–448. https://doi.org/10.1097/00004647-200404000-00009
49. Arvidsson A, Collin T, Kirik D, Kokaia Z, Lindvall O (2002) Neuronal replacement from endogenous precursors in the adult brain after stroke. Nat Med 8(9):963–970
50. Zhang RL, Chopp M, Roberts C, Jia L, Wei M, Lu M, Wang X, Pourabdollah S et al (2011) Ascl1 lineage cells contribute to ischemia-induced neurogenesis and oligodendrogenesis. Journal of Cerebral Blood Flow and Metabolism: Official Journal of the International Society of Cerebral Blood Flow and Metabolism 31(2):614–625. https://doi.org/10.1038/jcbfm.2010.134
51. Benner EJ, Luciano D, Jo R, Abdi K, Paez-Gonzalez P, Sheng H, Warner DS, Liu C et al (2013) Protective astrogenesis from the SVZ niche after injury is controlled by Notch modulator Thbs4. Nature 497(7449):369–373. https://doi.org/10.1038/nature12069
52. Faiz M, Sachewsky N, Gascon S, Bang KW, Morshead CM, Nagy A (2015) Adult neural stem cells from the subventricular zone give rise to reactive astrocytes in the cortex after stroke. Cell Stem Cell 17(5):624–634. https://doi.org/10.1016/j.stem.2015.08.002
53. Tavazoie M, Van der Veken L, Silva-Vargas V, Louissaint M, Colonna L, Zaidi B, Garcia-Verdugo JM, Doetsch F (2008) A specialized vascular niche for adult neural stem cells. Cell Stem Cell 3(3):279–288. https://doi.org/10.1016/j.stem.2008.07.025
54. Yamashita T, Ninomiya M, Hernandez Acosta P, Garcia-Verdugo JM, Sunabori T, Sakaguchi M, Adachi K, Kojima T et al (2006) Subventricular zone-derived neuroblasts migrate and differentiate into mature neurons in the post-stroke adult striatum. The Journal of Neuroscience: the Official Journal of the Society for Neuroscience 26(24):6627–6636
55. Li L, Harms KM, Ventura PB, Lagace DC, Eisch AJ, Cunningham LA (2010) Focal cerebral ischemia induces a multilineage cytogenic response from adult subventricular zone that is predominantly gliogenic. Glia 58(13):1610–1619. https://doi.org/10.1002/glia.21033
56. Guo F, Maeda Y, Ma J, Xu J, Horiuchi M, Miers L, Vaccarino F, Pleasure D (2010) Pyramidal neurons are generated from oligodendroglial progenitor cells in adult piriform cortex. The Journal of Neuroscience: the Official Journal of the Society for Neuroscience 30(36):12036–12049. https://doi.org/10.1523/JNEUROSCI.1360-10.2010
57. Rivers LE, Young KM, Rizzi M, Jamen F, Psachoulia K, Wade A, Kessaris N, Richardson WD (2008) PDGFRA/NG2 glia generate myelinating oligodendrocytes and piriform projection neurons in adult mice. Nat Neurosci 11(12):1392–1401. https://doi.org/10.1038/nn.2220
58. Salmaso N, Silbereis J, Komitova M, Mitchell P, Chapman K, Ment LR, Schwartz ML, Vaccarino FM (2012) Environmental enrichment increases the GFAP+ stem cell pool and reverses hypoxia-induced cognitive deficits in juvenile mice. The Journal of Neuroscience: the Official Journal of the Society for Neuroscience 32(26):8930–8939. https://doi.org/10.1523/JNEUROSCI.1398-12.2012
59. Honsa P, Pivonkova H, Dzamba D, Filipova M, Anderova M (2012) Polydendrocytes display large lineage plasticity following focal cerebral ischemia. PLoS One 7(5):e36816. https://doi.org/10.1371/journal.pone.0036816
60. Soderholm M, Almgren P, Jood K, Stanne TM, Olsson M, Ilinca A, Lorentzen E, Norrving B et al (2016) Exome array analysis of ischaemic stroke: results from a southern Swedish study. European Journal of Neurology: the Official Journal of the European Federation of Neurological Societies 23(12):1722–1728. https://doi.org/10.1111/ene.13086